

# Protein–Protein Interactions in Ovalbumin Solutions Studied by Small-Angle Scattering: Effect of Ionic Strength and the Chemical Nature of Cations

Luca Ianeselli,<sup>†</sup> Fajun Zhang,<sup>\*,†</sup> Maximilian W. A. Skoda,<sup>‡</sup> Robert M. J. Jacobs,<sup>§</sup> Richard A. Martin,<sup>||</sup> Shirley Callow,<sup>⊥</sup> Sylvain Prévost,<sup>#</sup> and Frank Schreiber<sup>†</sup>

*Institut für Angewandte Physik, Universität Tübingen, Auf der Morgenstelle 10, 72076 Tübingen, Germany, ISIS, Rutherford Appleton Laboratory, Chilton, Didcot, OX11 0QX, United Kingdom, Department of Chemistry, Chemistry Research Laboratory, University of Oxford, Mansfield Road, OX1 3TA, United Kingdom, Aston Research Centre for Healthy Ageing, Aston University, Aston Triangle, Birmingham, B4 7ET, United Kingdom, European Synchrotron Radiation Facility, 6 rue Jules Horowitz, F-38043 Grenoble Cedex 9, France, and Helmholtz Center Berlin, Glienicker Strasse 100, 14109 Berlin, Germany*

Received: November 25, 2009; Revised Manuscript Received: February 17, 2010

The influence of ionic strength and of the chemical nature of cations on the protein–protein interactions in ovalbumin solution was studied using small-angle X-ray and neutron scattering (SAXS/SANS). The globular protein ovalbumin is found in dimeric form in solutions as suggested by SANS/SAXS experiments. Due to the negative charge of the proteins at neutral pH, the protein–protein interactions without any salt addition are dominated by electrostatic repulsion. A structure factor related to screened Coulombic interactions together with an ellipsoid form factor was used to fit the scattering intensity. A monovalent salt (NaCl) and a trivalent salt (YCl<sub>3</sub>) were used to study the effect of the chemical nature of cations on the interaction in protein solutions. Upon addition of NaCl, with ionic strength below that of physiological conditions (150 mM), the effective interactions are still dominated by the surface charge of the proteins and the scattering data can be understood using the same model. When yttrium chloride was used, a reentrant condensation behavior, i.e., aggregation and subsequent redissolution of proteins with increasing salt concentration, was observed. SAXS measurements reveal a transition from effective repulsion to attraction with increasing salt concentration. The solutions in the reentrant regime become unstable after long times (several days). The results are discussed and compared with those from bovine serum albumin (BSA) in solutions.

## Introduction

Nonspecific protein–protein interactions in solution attract much attention due to their direct relation to protein crystallization and protein association related diseases.<sup>1–4</sup> Protein crystallization has long been performed mostly using a trial-and-error method, partly due to the poor understanding of physicochemical conditions in their solutions.<sup>5</sup> In many cases, crystallization of a given protein needs extreme conditions that are far away from the physiological ones. In order to grow protein crystals, a widely adopted method is to use poly(ethylene glycol) (PEG), saturated ammonium sulfate, and pH variations.<sup>5</sup> The addition of PEG can provide a short-range attractive interaction between proteins through depletion, and concentrated ammonium sulfate reduces their solubility (salting-out effect). Tuning the pH of the solution close to the isoelectric point of the protein also reduces the long-range electrostatic repulsion. Although the role of these additives for protein crystallization has been known for quite a long time, they do not always work, and in many cases, instead of obtaining crystallized proteins, amorphous aggregates may appear or the solutions can form gels. Therefore, the control of not only the range but also the

strength of the attractive interactions between protein molecules in solution is crucial.

A quantitative description of these interactions is essential for establishing the relationship between the solution conditions and the final phase behavior. George and Wilson found out that proteins can crystallize within a narrow window of the second virial coefficient,  $A_2$ , which can therefore be used to predict the possibility of protein crystallization.<sup>6</sup>  $A_2$  describes the overall interactions between protein molecules without knowledge of the specific interactions.<sup>7,8</sup> Recent studies on protein–protein interactions using scattering techniques take advantage of colloidal science and liquid state theories.<sup>3,9–19</sup> Specific interactions, such as the screened Coulomb potential, van der Waals, sticky-hard sphere, and excluded-volume (hard sphere) interactions, can be modeled and compared with the experimental data.

We have recently studied the effects of ionic strength and ion valency on the phase behavior and interactions of a model protein: bovine serum albumin (BSA).<sup>20,21</sup> At neutral pH, this protein is negatively charged,  $-11e$ , and the charge dominates the effective protein–protein interactions in solution. SAXS studies for protein solutions without added salt give a pronounced correlation peak due to the long-range electrostatic repulsion. This charge induced interaction is very sensitive to the ionic strength of the solution, for a given protein concentration (say 100 mg/mL); upon increasing the ionic strength from 0 to 100 mM, the correlation peak gradually reduces.<sup>20</sup> When using trivalent ions, i.e., yttrium chloride, a reentrant phase behavior was observed.<sup>21</sup>

\* Corresponding author. E-mail: fajun.zhang@uni-tuebingen.de. Phone: +49-7071-2978670. Fax: +49-7071-295110.

<sup>†</sup> Universität Tübingen.

<sup>‡</sup> Rutherford Appleton Laboratory.

<sup>§</sup> University of Oxford.

<sup>||</sup> Aston University.

<sup>⊥</sup> European Synchrotron Radiation Facility.

<sup>#</sup> Helmholtz Center Berlin.

In this work, we study another globular protein: ovalbumin from chicken egg white (OV). Although it possesses a very similar net charge at neutral pH, OV, in contrast to BSA, has a very different amount of solvent-accessible hydrophobic surface. Moon et al. and Anderson et al. calculated the solvent-accessible hydrophobic area for ovalbumin and human serum albumin (HSA), and they found values of 19 and 9%, respectively.<sup>22,23</sup> Furthermore, the HSA surface is more hydrophobic than BSA because the former presents hydrophobic-surface residues that do not have a counterpart in BSA.<sup>22</sup> As a consequence, the surface of ovalbumin is significantly more hydrophobic than the surface of BSA.<sup>22,23</sup> It is therefore interesting to compare the protein–protein interactions in solution of these two proteins as a function of ionic strength and ion valency, and this is the focus of this work. By means of SAXS, SANS, and other techniques, we present an analysis of the protein–protein interactions as a function of ionic strength and protein concentration. A monovalent salt (NaCl) and a trivalent salt (YCl<sub>3</sub>) were selected to study the effect of the chemical nature of cations on the interactions as well as the phase behavior.

Ovalbumin is present in many biological systems and is widely used in the food industry.<sup>24,25</sup> Many studies have been performed in order to interrogate the molecule–molecule interactions for OV. Weijers et al., for instance, studied the dependency of the interactions on the ionic strength in solution, while other authors studied the aggregation phenomena of OV under temperature induced denaturation.<sup>26–28</sup> These results indicate that, due to their negative net charge at neutral pH, the interactions between OV molecules in solution are dominated by electrostatics. OV is a medium size globular protein with a molar mass of 45 kDa and 385 amino acid residues. In the crystal structure, OV presents itself as a slightly elongated ellipsoid with dimensions of 70 × 45 × 50 Å<sup>3</sup> which yield an effective spherical diameter of 50 Å.<sup>29</sup> In solution, it forms dimers with a radius of gyration of about 27 Å, which does not depend on the ionic strength, as measured using small-angle X-ray scattering.<sup>30,31</sup> Ovalbumin has an isoelectric point of 4.9. At neutral pH (pH 7), OV possesses an absolute negative charge of about −11e, which is very similar to that on BSA.<sup>23,32</sup>

This Article is divided into two parts. In the first part, we study protein solutions with and without the addition of monovalent salts (e.g., NaCl), comparing our results with the literature. In the second part, we study the effect of a trivalent salt, YCl<sub>3</sub>, on the protein–protein interactions and phase diagram of the solution. Similarities and differences in protein interactions and phase behavior compared with BSA are discussed.

## 2. Experimental Section

**2.1. Materials.** Albumin from chicken egg white, OV (A5503), was purchased from Sigma-Aldrich and delivered as a lyophilized powder at 98% purity and a molecular weight of ~45 kDa. No further purification was performed. NaCl, NaSCN, Na<sub>2</sub>SO<sub>4</sub>, and YCl<sub>3</sub> were equally purchased from Sigma Aldrich at high-purity grade (>99%). Milli-Q water was used to prepare all solutions, unless otherwise stated.

Stock solutions for the protein (OV 200 mg/mL) and the salts (salt concentration 200 mM) were prepared and then diluted in order to obtain the desired concentrations. The protein stock solution was further filtered through 0.22 μm membrane filters (Millipore). For SANS measurements, D<sub>2</sub>O (99.9%, Aldrich) was used instead of H<sub>2</sub>O to lower the incoherent scattering and the absorption, and increase the contrast with the protein. In order to study only the effect of the salt in the protein–protein

interactions, no buffer was used. The pH of the solution was ~7.0 and did not change significantly by varying the protein concentration and adding NaCl. All of the solutions were prepared and studied at room temperature.

**2.2. Circular Dichroism.** Circular dichroism (CD) spectroscopy was used to study the secondary structure of the OV molecules in solution as a function of the ionic strength (using YCl<sub>3</sub>). The measurements were carried out at room temperature using a CD-810 instrument from JASCO (wavelength range 200–250 nm) with a quartz cell of 0.1 cm path length and a scanning speed of 200 nm/min. In order to subtract the water background, a preliminary spectrum for water was collected and then automatically subtracted from each solution spectrum.

**2.3. Small-Angle X-ray Scattering.** The SAXS measurements were performed at the ESRF (Grenoble, France) on the beamline ID02 with a sample-to-detector distance of 2 m.<sup>33</sup> The wavelength of the incoming beam was 1.127 Å (11.0 keV), covering a *q* range of 0.005–0.21 Å<sup>−1</sup>. Additional data (Figure 2a, right) were collected at 16.038 keV with a *q* range of 0.006–0.42 Å<sup>−1</sup>. The data were collected by a high-sensitivity fiber-optic coupled CCD (FReLoN) detector placed in an evacuated flight tube. The protein solutions were loaded using a flow-through capillary cell (diameter ~2 mm; wall thickness ~50 μm). No variation of SAXS profiles was observed due to radiation damage during 10 successive exposures of 0.3 s. The incident and transmitted beam intensities were simultaneously recorded with each SAXS pattern with exposure of 0.3 s. The 2D data were normalized to an absolute scale and azimuthally averaged to obtain the intensity profiles, and the solvent background was subtracted. For more detailed information on data reduction and *q*-resolution calibration, see ref 34.

Some data (Figure 6a) were collected at station 6.2 of the Synchrotron Radiation Source (SRS) at the Daresbury Laboratory, Warrington, U.K. The detailed data correction and calibration has been described in previous publications.<sup>20,35</sup>

**2.4. Small-Angle Neutron Scattering.** Small-angle neutron scattering (SANS) measurements were performed on the SANS instrument V4 at the Helmholtz Center, Berlin, Germany.<sup>36</sup> Three configurations were used with sample-to-detector (SD) distances of 1, 4, and 12 m and collimation lengths of 8, 4, and 12 m, respectively, in order to cover the *q* range from 0.005 to 0.35 Å<sup>−1</sup> at a wavelength of 6 Å. The data were recorded on a 64 × 64 cm<sup>2</sup> two-dimensional detector and radially averaged and converted into absolute units by comparison with the scattering of a 1 mm H<sub>2</sub>O sample and corrected for the detector background and scattering of the empty cell. The data reduction was performed using the software BerSANS.<sup>37</sup> Protein solutions in D<sub>2</sub>O were filled in quartz cells with a path length from 5 to 10 mm.

**2.5. Data Analysis.** The scattering intensity, *I*, for a poly-dispersed or a nonspherical system, can be calculated on the basis of approximation approaches. Most often used are the “decoupling approximation” and “average structure factor” approximation.<sup>38,39</sup> Both approaches assume that the particle position is not correlated with its orientation. As the particles become more anisotropic or more concentrated, this approximation becomes less precise. In the case of nonspherical but monodisperse systems, such as proteins in solution, both assumptions give similar results. Therefore, in this work, the scattering intensity is calculated using the *average structure factor* approximation, which can be expressed by<sup>38,40–42</sup>

$$I(q) = N_p(\Delta\rho)^2 V_p^2 P(q) \bar{S}(q) \quad (1)$$

where  $q = 4\pi \sin \theta/\lambda$ ,  $2\theta$  denotes the scattering angle,  $N_p$  is the number of protein molecules per unit volume in the solution,  $V_p$  is the volume of a single protein, and  $\Delta\rho = (\rho_p - \rho_s)$  is the scattering contrast.  $P(q)$  is the form factor of a given protein, i.e., the scattering from a single protein molecule after orientation averaging. An ellipsoid form factor was used to model ovalbumin.

$$P(q) \equiv \langle |F(q)|^2 \rangle = \int_0^1 dx \left| \frac{3(\sin u - u \cos u)}{u^3} \right|^2 \quad (2)$$

$$u = qb[(a/b)^2 x^2 + (1-x)^2]^{1/2}$$

For a dilute protein solution, where protein molecules are well dispersed, the interaction between them is negligible. In this case, the scattering intensity is the summation of the scattering intensities of all of the proteins within the illuminated volume. At the sufficient low- $q$  range ( $qR_g < 1$ ), the scattering intensity can be approximated by Guinier law:<sup>41,43</sup>

$$\ln I(q) = \ln I(0) - \frac{1}{3} R_g^2 q^2 \quad (3)$$

where  $I(0)$  is the forward scattering at zero angle and  $R_g$ , the radius of gyration. Equation 3 provides a direct method to determine  $R_g$ . In practice, eq 3 can be valid in the range of  $qR_g$  up to 1.5.<sup>44</sup>

Under the average structure factor approximation,  $\bar{S}(q)$  is calculated using a monodisperse structure factor with an effective sphere diameter. In our case, the protein solution is a monodisperse but nonspherical (ellipsoidal) system. The effective sphere diameter is calculated by equating the second virial coefficient,  $A_2$ , of the ellipsoid to a sphere having the same  $A_2$ . This effective diameter is then used to calculate  $\bar{S}(q)$ .<sup>20,21,45</sup> In the remaining part of the paper, we use  $S(q)$  to represent  $\bar{S}(q)$ .

At lower ionic strength (<100 mM), the protein is negatively charged and the charge induced interaction can be described using the screened Coulombic potential developed by Hayter and Penfold.<sup>46,47</sup> The model is based on an interaction potential  $U_{SC}(r)$  between charged colloidal particles consisting of a hard sphere plus a screened Coulomb potential.

$$U_{SC}(r) = \begin{cases} \frac{z^2 e^2}{\varepsilon(1 + \kappa_D R)^2} \frac{\exp[-\kappa_D(r - 2R)]}{r} & \text{for } r > 2R \\ \infty & \text{for } r \leq 2R \end{cases} \quad (4)$$

The charge of the protein,  $z$ , is assumed to be uniformly distributed on the surface,  $e$  is the electronic charge, and  $\varepsilon$  is the dielectric constant of the solvent.  $\kappa_D$  is the inverse of the Debye screening length and is determined by the ionic strength,  $I_{ion}$ , of the solution.

$$\kappa_D^{-1} = \frac{\varepsilon \varepsilon_0 RT}{2\rho F^2 I_{ion}} \quad (5)$$

where  $\varepsilon = 80.1$ ,  $\varepsilon_0 = 8.85 \times 10^{-12} \text{ J}^{-1} \text{ C}^2 \text{ m}^{-1}$ ,  $R = 8.314 \text{ J K}^{-1} \text{ mol}^{-1}$ ,  $T = 293 \text{ K}$ ,  $\rho = 1000 \text{ kg m}^{-3}$ , and  $F = 96458 \text{ C mol}^{-1}$ .

The data analysis was carried out using macros developed by the NIST center for neutron scattering research.<sup>45</sup>

### 3. Results and Discussion

**3.1. Scattering from Dilute Protein Solutions: Form Factor.** Small-angle X-ray and neutron scattering data of selected samples with low protein concentrations were collected (Figure 1a and c). Under these conditions, the protein–protein correlations in solution are negligible and thus the structure factor in eq 1 equals 1. The Guinier approximation (eq 3) in practice can be valid in the range of  $qR_g$  up to 1.5.<sup>44</sup> The corresponding Guinier plots (Figure 1b and d) were fitted in the  $q^2$  range 0.0002–0.002  $\text{\AA}^{-2}$ . A summary of the  $R_g$  values determined by Guinier analysis for both SAXS and SANS is listed in Table 1. SAXS measurements give  $R_g = 28 \pm 1 \text{ \AA}$ , in good agreement with the reported values where the proteins form dimers in solution.<sup>30</sup> In the case of SANS, the  $R_g$  values are systematically smaller by about 4–5  $\text{\AA}$ . This difference is due to the contribution of the hydration shell of proteins. Since the SANS signal mainly arises from the coherent scattering of protons in proteins due to the large difference between the H and D scattering lengths ( $-0.374 \times 10^{-12} \text{ cm}$  for H and  $0.667 \times 10^{-12} \text{ cm}$  for D), the contribution from the hydrated  $\text{D}_2\text{O}$  layer is negligible.<sup>48</sup> SANS thus probes the “dry” protein without “seeing” the hydration shell, whereas SAXS probes the whole complex due to the difference of electron density in the hydration shell compared to the bulk solution.<sup>48</sup>

Further structural information of proteins was obtained by fitting the experimental scattering curves using an ellipsoidal form factor. The fitting results give an average value of  $R_a = 57 \pm 2 \text{ \AA}$  and  $R_b = 21 \pm 2 \text{ \AA}$  for the SAXS data. Protein crystallography studies have shown that the ovalbumin molecule can be described by an ellipsoid with radii of  $R_a = 35 \text{ \AA}$  and  $R_b = 25 \text{ \AA}$ .<sup>29</sup> The elongation in  $R_a$  is due to the dimerization. Similar results have been observed by Matsumoto and Chiba.<sup>30</sup> In the concentration range from 0.5 to 20 mg/mL, our SAXS/SANS data can be fitted using an ellipsoid form factor with an elongated  $R_a$ , suggesting that the proteins form dimers in all cases.

**3.2. Protein–Protein Interactions: Effect of Protein Concentration and Ionic Strength.** With the knowledge of the form factor, i.e., the scattering from a single protein molecule, the effective protein–protein interaction in solutions with higher concentrations can be studied by SAXS. We first studied the interactions for pure protein solutions as a function of concentration (Figure 2). A maximum scattering intensity is clearly visible for all of the protein solutions from 20 to 200 mg/mL (Figure 2a, left). The position of this peak shifts to higher  $q$  values with increasing protein concentration. Ovalbumin is negatively charged at neutral pH with a net charge of  $-11e$ .<sup>23,32</sup> This correlation peak thus characterizes the dominating electrostatic repulsion between the charged protein molecules. The shifting to higher  $q$ -values for higher protein concentrations indicates the reduced average distance between the protein molecules in solution.

The charge induced protein–protein interactions can be described using a screened Coulombic potential.<sup>20</sup> SAXS data were fitted using an ellipsoidal form factor combined with a screened Coulombic structure factor developed by Hayter and Penfold.<sup>46</sup> The model fits (plotted as solid lines in Figure 2a) agree very well with the scattering curves in the region of the correlation peak. The fit parameters include volume fraction ( $\phi$ ), ionic strength ( $I_{ion}$ ), and surface charge ( $z$ ). Other parameters including  $R_a = 57 \text{ \AA}$ ,  $R_b = 21 \text{ \AA}$ ,  $T = 293 \text{ K}$ ,  $\varepsilon = 80.1$ , and a

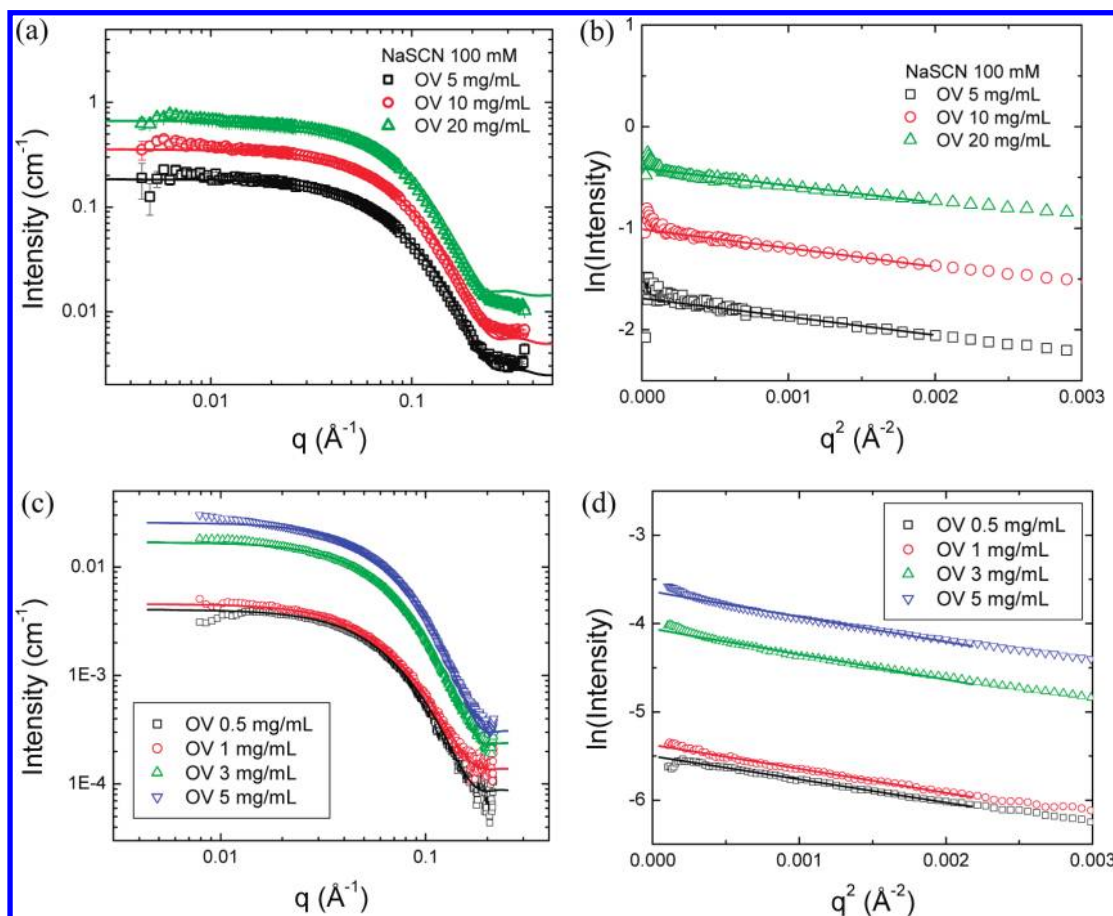


**Figure 1.** SANS and SAXS data (scattered points) with model fitting (lines) for ovalbumin solutions with 100 mM NaSCN and (b) corresponding Guinier plots; (c) SAXS data of four diluted ovalbumin solutions with 150 mM NaCl and (d) corresponding Guinier plots. The Guinier plots were fitted in the  $q^2$  range  $0.2$  to  $2 \times 10^{-3}$  Å<sup>-2</sup>.

**TABLE 1: Radius of Gyration,  $R_g$ , of Ovalbumin Solutions with Various Salts Studied by SAXS and SANS**

SAXS		SANS	
OV_NaCl 150 mM	$R_g$ (Å)	OV solutions	$R_g$ (Å)
0.5 mg/mL	$28 \pm 1$	5 mg/mL NaCl 100 mM	$25 \pm 1$
1 mg/mL	$28 \pm 1$	20 mg/mL NaCl 100 mM	$24 \pm 1$
3 mg/mL	$29 \pm 1$	5 mg/mL NaSCN 100 mM	$25 \pm 1$
5 mg/mL	$29 \pm 1$	10 mg/mL NaSCN 100 mM	$24 \pm 1$
		20 mg/mL NaSCN 100 mM	$21 \pm 1$
		5 mg/mL Na <sub>2</sub> SO <sub>4</sub> 33.3 mM	$24 \pm 1$
		10 mg/mL Na <sub>2</sub> SO <sub>4</sub> 33.3 mM	$24 \pm 1$
		20 mg/mL Na <sub>2</sub> SO <sub>4</sub> 33.3 mM	$24 \pm 1$

constant background are fixed during data fitting. The fitted contrast varies from  $0.8$  to  $3 \times 10^{10}$  cm<sup>-2</sup> for data collected from different sources. This variation may be due to the absolute intensity calibration. The errors of the fitting parameters (listed in Table 2) pertaining to the fitting procedure are better than 5%, but the systematic errors, including sample preparation, raw data correction, and calibration, are estimated to be  $\sim 10\%$ .<sup>20</sup> A typical fit for a sample solution with 100 mg/mL gives  $\phi = 9.58\%$ ,  $z = 11.6e$ , and  $I_{\text{ion}} = 0.0016$  M. The fitting results are consistent with the sample solution after filtration, which gives  $\phi = 11.0\%$ ,  $z = 9.4e$ , and  $I_{\text{ion}} = 0.008$  M. In both cases, the net charge is determined to be around  $10e$ , which is an absolute value, in good agreement with the net charge of ovalbumin at neutral pH ( $-11e$ ). The fitted volume fraction ( $\phi \sim 10\%$ ) is higher than the value ( $\phi \sim 7.55\%$ ) calculated on the basis of sample preparation. Although no salt was added into protein solutions, the fitted ionic strength is below 10 mM which comes

from the dissociation of charged groups on the protein surface. Similar trends were also observed for BSA.<sup>20</sup> We have also noticed that the fitted ionic strength for solutions without filtration is slightly high ( $>0.01$  M), which corresponds to a higher charge value. When we fix  $I_{\text{ion}} = 0$ , the charge ( $\sim 8$ ) is determined to be consistent with the results from the filtered samples. Both sets of fitting results are listed in Table 2.

In the low- $q$  range, the experimental data show a strong increase which the fit procedure cannot reproduce. In order to clarify the origin of the low- $q$  scattering behavior, we have repeated several measurements with a larger  $q$  range (Figure 2a, right). The sample solutions are freshly prepared and filtered using  $0.1 \mu\text{m}$  membrane filters. The low- $q$  upturn is significantly but not completely reduced. Model fits agree very well with SAXS data. The fits to the second scattering maximum at  $q \sim 0.25$  Å<sup>-1</sup> indicate the ellipsoid form factor describes the globular shape of protein very well. The low- $q$  upturn of scattering intensity has been observed in many protein solution systems; however, so far, there is no general explanation for this phenomenon.<sup>12,13,15,49,50</sup> Liu et al. for instance, propose the existence of a long-range attraction, which could account for the upturn in the low- $q$  region.<sup>12</sup> On the other hand, the low- $q$  upturn was also found to depend on sample preparation, purity of protein product, and aging.<sup>49</sup> A theoretical study by Sciortino et al. indicates that a combination of short-range attraction and long-range repulsion can result in the formation of equilibrium clusters in a colloidal system.<sup>50</sup> Stradner et al. claim the formation of equilibrium clusters in lysozyme solution as well as colloidal solution when controlling the interactions carefully.<sup>15</sup>

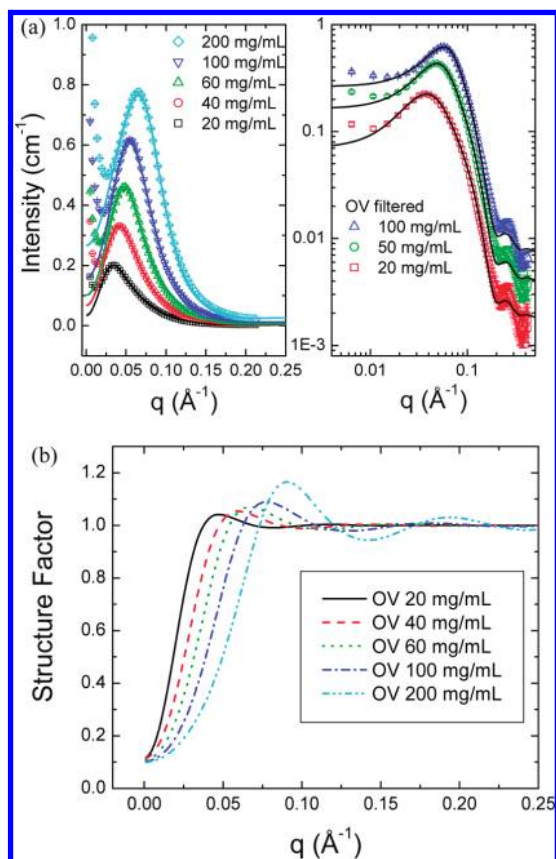


**Figure 2.** (a) SAXS data with model fit of ovalbumin solutions with concentrations from 20 to 200 mg/mL without added salt: (left) sample solutions without filtration; (right) sample solutions filtered with 0.1  $\mu\text{m}$  filters. Only every fifth data point is shown for clarity. (b) The screened Coulombic structure factor  $S(q)$  evaluated from data fitting in the  $q$  range 0.025–0.2  $\text{\AA}^{-1}$ .

**TABLE 2: Fitting Parameters of SAXS Data Using an Ellipsoid Form Factor Plus a Screened Coulomb Structure Factor<sup>a</sup>**

sample	$\phi$ (%)	fitted $\phi$	charge ( $e$ )	$I_{\text{ion}}$ (M)
20 mg/mL	1.38	1.46/1.56	13.4/7.9	0.005/0
40 mg/mL	2.97	3.21/3.68	14.9/7.7	0.011/0
60 mg/mL	4.65	5.49/6.13	14.2/8.0	0.015/0
80 mg/mL	6.13	6.97/7.64	13.3/7.9	0.016/0
100 mg/mL	7.55	9.58/10.1	11.6/7.8	0.016/0
140 mg/mL	10.1	13.5/13.4	9.9/7.3	0.017/0
200 mg/mL	14.5	17.7/16.8	7.4/6.3	0.016/0
20 mg/mL filtered	1.38	2.49	8.7	0.001
50 mg/mL filtered	3.62	6.08	9.6	0.004
100 mg/mL filtered	7.55	11.0	9.4	0.008
OV100 NaCl 0.01 M	8.42/8.74	11.5/8.2	0.026/0.01	
OV100 NaCl 0.02 M	7.78/8.32	16.7/7.3	0.098/0.02	
OV100 NaCl 0.05 M	8.45/8.85	13.2/6.8	0.136/0.05	
OV100 NaCl 0.10 M	7.32/7.70	21.0/6.8	0.418/0.10	
OV20 $\text{YCl}_3$ 0.4 mM	1.01	6.6	0.002	
OV20 $\text{YCl}_3$ 0.6 mM	1.25	3.2	0.005	
OV20 $\text{YCl}_3$ 0.8 mM	1.79	0.015	0.011	

<sup>a</sup>The error of the fitting parameters pertaining to the fitting procedure are better than 5%, but the systematic errors, including sample preparation, raw data correction, and calibration, are estimated to be  $\sim 10\%$ .

However, the result presented by Shukla et al. indicated that the equilibrium clusters in lysozyme solution are still challenging to understand.<sup>13</sup> The sample solutions used in this work have been centrifuged before the measurements, but because of the hydrophobic property of ovalbumin, further aggregation might

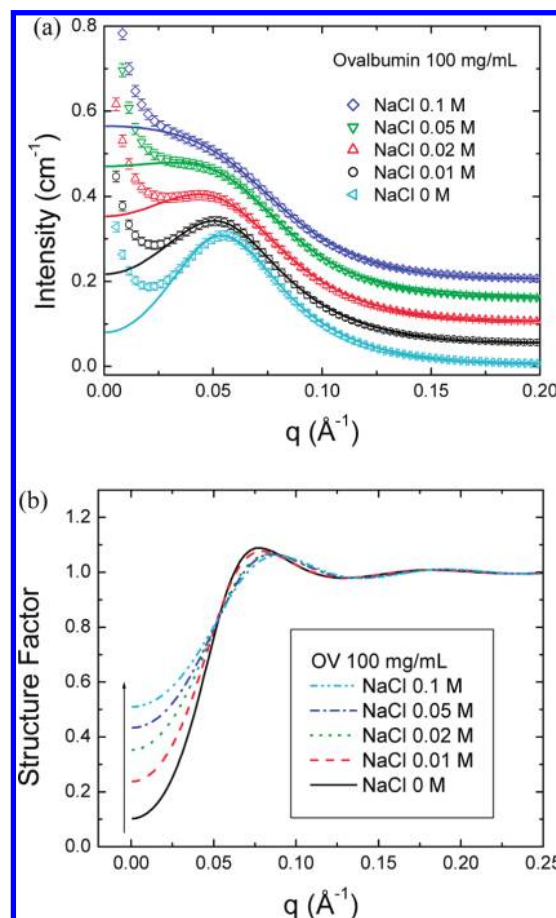


**Figure 3.** (a) SAXS profiles of ovalbumin solutions (100 mg/mL) with different ionic strengths; the data were shifted upward for clarity. (b) The structure factors evaluated from data analysis. Note that the data were fit in the range 0.025–0.2  $\text{\AA}^{-1}$ .

have occurred during the measurement due to the short-range hydrophobic attraction. Therefore, we do not intend to fit this feature of the scattering profile in this work. The structure factors,  $S(q)$ , evaluated from data fitting are plotted in Figure 2b. The first peak of  $S(q)$  not only shifts to high  $q$  but also increases its intensity with protein concentration, indicating the enhanced repulsive interaction with increasing protein concentration. Comparing to the results obtained with BSA,<sup>20</sup> we can state that in both cases the surface charge dominates the effective interactions in the protein solutions. The difference is that, for ovalbumin, protein clusters can be easily formed due to the hydrophobic property of ovalbumin, while, for BSA, the screened Coulombic potential fits the data very well.<sup>20</sup>

For further investigation on the nature of the interactions, we measured a series of solutions with fixed protein concentration but varied the ionic strength using NaCl. The collected scattering curves are shown in Figure 3a. With increasing ionic strength, the correlation peak decreases and disappears completely at  $I_{\text{ion}} = 100$  mM. This strong ionic strength dependence indicates the nature of charge-induced interactions. Increasing the ionic strength screens the surface charge and thus reduces the Debye length in eq 5. Fitting parameters without or with fixed  $I_{\text{ion}}$  are listed in Table 2. The charge values increase with increasing NaCl concentration. However, the fitted  $I_{\text{ion}}$  values are much higher than expected. When  $I_{\text{ion}}$  is fixed, the charge values are slightly reduced. Previous studies on BSA solutions show that the charge values increase with ionic strength and the fitted  $I_{\text{ion}}$  is very close to the added salt concentration.<sup>20</sup> The scattering intensity increase in the low- $q$  region can still be seen

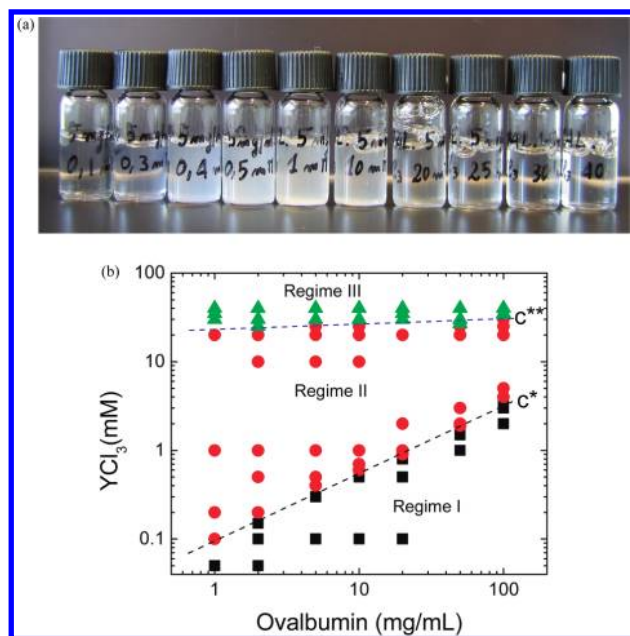


**Figure 4.** (a) Digital images of a series of protein solutions (5 mg/mL) as a function of yttrium chloride concentration; reentrant phase behavior was observed. (b) Phase diagram as a function of protein and salt concentration with logarithmic axes. The lines for  $c^*$  and  $c^{**}$  are guides for the eye. Note that all phase behavior was determined within hours after sample preparation.

in this case, which can not be described using the screened Coulombic potential. The model is in good agreement with experimental data for the correlation peak as a function of increasing ionic strength. The structure factor evaluated from data fitting (Figure 3b) shows that the intensity at  $q = 0$  increases with ionic strength, indicating the reduced repulsive interaction.  $S(q)$  in the low- $q$  range strongly depends on the interaction potential between protein molecules. The structure factor at the origin  $S(q = 0)$  is equal to the normalized osmotic compressibility. With repulsive interactions, the protein molecules are uniformly distributed and  $S(0)$  is lower than unity, while, with attractive interactions, fluctuations dominate the particle distribution and  $S(0)$  is larger than unity.<sup>3,9</sup>

**3.3. Protein–Protein Interactions: Effect of Trivalent Cations. 3.3.1. Phase Diagram.** Series of ovalbumin solutions with different  $YCl_3$  concentrations were prepared. The phase state of the proteins in solution, either dissolved or condensed, was then established through optical inspection and laser transmission.<sup>21</sup> A typical photograph for ovalbumin 5 mg/mL as a function of salt concentration ( $YCl_3$ ) is presented in Figure 4a. The protein solutions are clear with low salt concentration ( $<0.4$  mM); with increasing salt concentration crossing  $c^* \sim 0.4$  mM, the protein solutions become turbid due to protein aggregation. When further increasing the salt concentration above  $c^{**} \sim 20$  mM, the protein solutions become clear again. This reentrant condensation phase behavior has been discovered recently by our group.<sup>21</sup> A phase diagram (Figure 4b) was collected as a function of protein and salt concentration within hours after sample preparation. The two transition concentrations,  $c^*$  and  $c^{**}$ , clearly divide the phase diagram into three regimes.

This reentrant phase behavior suggests the completely different response of protein–protein interactions and phase behavior to the high-valency ions in solution. Similar phase behavior has been observed in systems such as conventional colloids, DNA, and polyelectrolytes in the presence of multi-

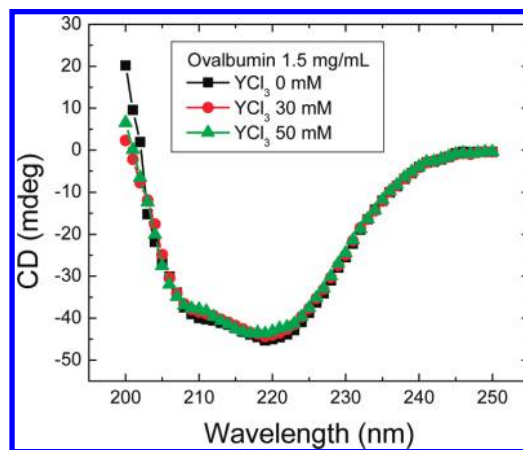


**Figure 5.** CD spectra of the protein solution (OV 1.5 mg/mL) without and with added  $YCl_3$ . No significant change in protein secondary structure was observed upon multivalent salt addition.

valent salts.<sup>51,52</sup> The electrostatic interactions under the strong electrostatic coupling condition (using multivalent ions) attract much attention due to the new phenomena presented, such as like-charge attraction, which cannot be explained using classical mean-field theories.<sup>53</sup> Although a complete theory is yet to be developed, such phase behavior can be explicitly explained by a charge inversion model. As suggested in our previous work<sup>21</sup> and supported also by Monte Carlo simulations, the cations ( $Y^{3+}$ ) can bind to the acidic residues on the protein surface, the number of bound ions gradually increasing with salt concentration. At an intermediate salt concentration, the binding ions neutralize the overall surface charge, and the proteins tend to aggregate because of the van der Waals and hydrophobic interactions. Upon further increase of the salt concentration, more cations can bind to the protein surface, which results in an effective inversion of the surface charge; i.e., the proteins become positively charged. The electrostatic repulsion again leads to the stabilization of protein solutions. This charge inversion effect has been confirmed using zeta-potential measurements on a series of proteins with multivalent salts (unpublished data).

It is worth noting that the protein secondary structure is preserved in the presence of  $Y^{3+}$  ions in solution. As shown in Figure 5, the two CD spectra of the protein in solution with and without yttrium chloride are in good agreement, indicating that the interaction of the  $Y^{3+}$  ions with proteins does not change the protein's native secondary structure.

Although the reentrant phase behavior occurs for both OV and BSA in the presence of trivalent cation, the stability of the solutions in the reentrant regime is different (regime III in Figure 4a). While the BSA solutions in the reentrant regime are stable for very long time (months), the ovalbumin solutions are not stable for a long time period (several days). Proteins begin to aggregate and solutions become turbid. The reason for this kinetically controlled phase behavior is not clear. The following SAXS experiments provide some clues to the answer to this question.

**3.3.2. Protein–Protein Interactions in the Presence of Trivalent Cations Studied by SAXS.** SAXS measurements were performed in order to understand the effective protein–protein interactions in the presence of the  $YCl_3$ . First, we studied protein solutions at salt concentrations  $c < c^*$  (Figure 6a,b); then, we moved on to solutions with salt concentrations  $c > c^{**}$  (Figure 6c). Here, the correlation peak depends, as in the case of NaCl, on the salt concentration. However, the screening effect of the

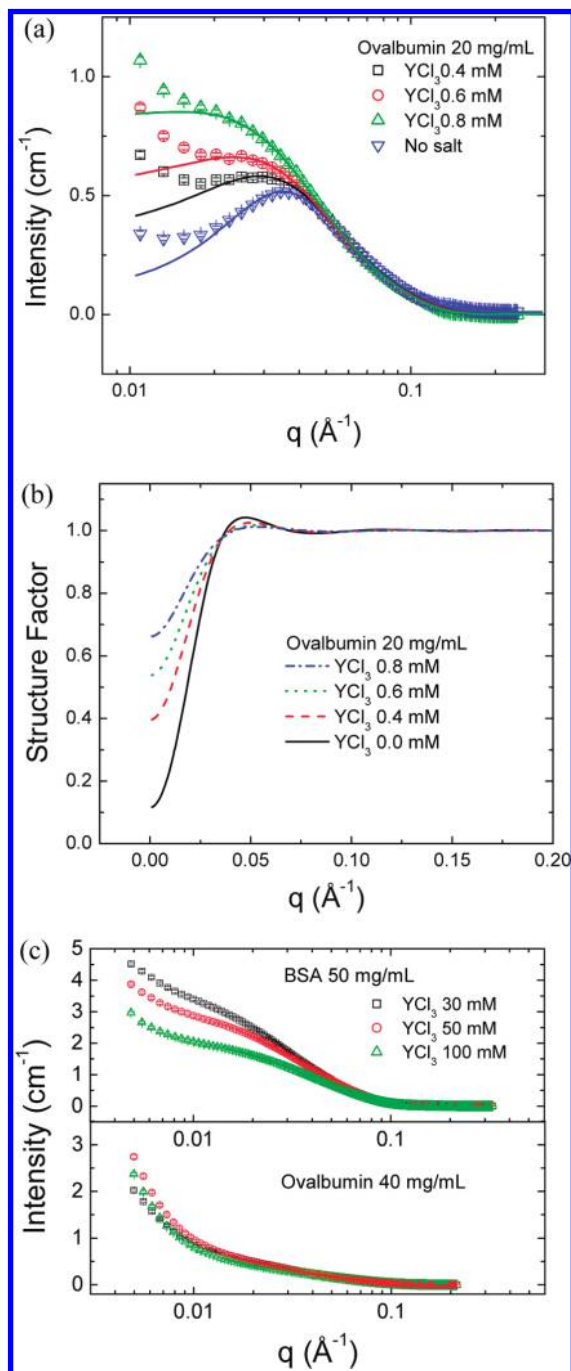


**Figure 6.** SAXS data for protein solutions with added multivalent salt: (a) SAXS data with model fitting in regime I,  $c < c^*$ ; (b) structure factors evaluated from the model fitting in part a; (c) comparison of SAXS data for ovalbumin (40 mg/mL) with BSA (50 mg/mL) with various YCl<sub>3</sub> concentrations in regime III,  $c > c^{**}$ .

trivalent salt is much stronger than that of the monovalent salt. With 0.8 mM yttrium chloride, the scattering maximum has almost disappeared. The SAXS data for solutions  $c < c^*$  can still be fitted using a screened Coulomb potential with an ellipsoid form factor, but the fit quality is poor due to the very small charge values (Table 2). The structure factors evaluated from the data fitting (Figure 6b) show a similar trend as the addition of NaCl (Figure 3b).

When  $c > c^{**}$ , the scattering profiles are different. Because the protein solutions in this regime were not stable for a long time, the SAXS measurements were performed immediately for freshly prepared samples after 30 min of centrifugation. Figure

6c (bottom) shows the SAXS profiles of ovalbumin 40 mg/mL with YCl<sub>3</sub> of 30, 50, and 100 mM. The scattering intensities increase significantly with decreasing  $q$  values, indicating that the overall interactions are dominated by attractive potentials. Small amounts of white precipitates were observed from the sample solutions after centrifugation, indicating the formation of protein clusters driven by the attractive potential. In this case, the form factor is different from the monodispersed protein solutions and the interactions cannot be explained by charge interactions alone. Thus, we have not applied this model to the data. It is interesting to compare the data of BSA and ovalbumin under the same conditions (Figure 6c). While the low- $q$  intensity for ovalbumin increases slightly with salt concentration (meaning stronger aggregation), the scattering curves for BSA show a systematic decrease with salt concentration, indicating a reduced attractive interaction.<sup>21</sup> These differences make BSA solutions more stable than ovalbumin in the reentrant regime.

The reason for the variation in stability of BSA and ovalbumin in the reentrant regime is still not clear, but the difference between the proteins gives some clues. As described in the Introduction section, ovalbumin is more hydrophobic than BSA. The hydrophobic effect leads to protein aggregation, which could be responsible for the low- $q$  upturn in the SAXS data (Figures 2a and 3a) and also the reason for the unstable reentrant regime. On the other hand, the binding of Y<sup>3+</sup> on the protein surface is due to the strong associated effect between cations and the carboxyl group of the acidic residues on the protein surface.<sup>21</sup> Therefore, the number of the acidic residues plays a very important role in the reentrant phase behavior. BSA has 583 residues in total, which includes 99 acidic residues. Ovalbumin has 385 residues in total with 47 acidic residues. This difference of the binding sites on the protein surface is also a potential reason for the instability of ovalbumin solutions.

#### 4. Conclusions

We have studied the interactions of proteins (ovalbumin) in solution using small-angle scattering, and the effects of ionic strength and valency were addressed. Ovalbumin in solution forms dimers at all of the studied concentrations, and the form factor can be described by using an ellipsoid with  $R_a = 57 \pm 2$  Å and  $R_b = 21 \pm 2$  Å. Without any salt addition, the effective protein-protein interaction with protein concentrations above 10 mg/mL is repulsive due to the net negative charge of acidic residues on the protein surface. This interaction can be described using a screened Coulombic potential. This repulsive interaction is significantly reduced by increasing the ionic strength of the solution. When trivalent salt (yttrium chloride) is added to the protein solutions, a reentrant phase behavior is observed on the experimental time scale (days). In the reentrant regime, the protein solutions become unstable after several days. This is in contrast to BSA, where the protein solutions are stable for much longer time scales. The SAXS data clearly present the difference: while the scattering intensity at low  $q$  for BSA decreases with increasing salt concentration, indicating the strengthening of repulsive interactions (which stabilizes the solutions), the low- $q$  intensity for ovalbumin solutions increases slightly with salt concentration, indicating a stronger aggregation. This difference may be due to the larger hydrophobic surface of ovalbumin compared to BSA.

**Acknowledgment.** We thank Dr. Avijit Pramanik of the Max-Planck Institute Tübingen for kind help with the CD measurement. We are grateful for the valuable discussions and comments from Dr. T. Narayanan (ESRF, Grenoble, France). We gratefully

acknowledge financial support from Deutsche Forschungsgemeinschaft (DFG) and the Engineering and Physical Sciences Research Council (EPSRC), U.K., and the beamtime allocation from CCLRC, ESRF, and Helmholtz-Center Berlin (BENSC). The beam time on V4 at the Helmholtz Zentrum Berlin has been supported by the European Commission under the sixth Framework Program through the Key Action: Strengthening the European Research Area, Research Infrastructures. Contract No. RII3-CT-2003-505925 (NMI3).

## References and Notes

- Piazza, R. *Curr. Opin. Colloid Interface Sci.* **2000**, *5*, 38.
- Piazza, R. *Curr. Opin. Colloid Interface Sci.* **2004**, *8*, 515.
- Tardieu, A.; Le Verge, A.; Malfois, M.; Bonneté, F.; Finet, S.; Riès-Kautt, M.; Belloni, L. *J. Cryst. Growth* **1999**, *196*, 193.
- Stradner, A.; Foffi, G.; Dorsaz, N.; Thurston, G.; Schurtenberger, P. *Phys. Rev. Lett.* **2007**, *99*, 198103.
- Durbin, S. D.; Feher, G. *Annu. Rev. Phys. Chem.* **1996**, *47*, 171.
- George, A.; Wilson, W. W. *Acta Crystallogr.* **1994**, *D50*, 361.
- Curtis, R. A.; Prausnitz, J. M.; Blanch, H. W. *Biotechnol. Bioeng.* **1998**, *57*, 11.
- Dumetz, A. C.; Snellinger-O'Brien, A. M.; Kaler, E. W.; Lenhoff, A. M. *Protein Sci.* **2008**, *16*, 1867.
- Bonneté, F.; Finet, S.; Tardieu, A. *J. Cryst. Growth* **1999**, *196*, 403.
- Häussler, W.; Wilk, A.; Gapinski, J.; Patkowski, A. *J. Chem. Phys.* **2002**, *117*, 413.
- Javid, N.; Vogt, K.; Krywka, C.; Tolan, M.; Winter, R. *ChemPhysChem* **2007**, *8*, 679.
- Liu, Y.; Fratini, E.; Baglioni, P.; Chen, W. R.; Chen, S. H. *Phys. Rev. Lett.* **2005**, *95*, 118102.
- Shukla, A.; Mylonas, E.; Di Cola, E.; Finet, S.; Timmins, P.; Narayanan, T.; Svergun, D. I. *Proc. Natl. Acad. Sci. U.S.A.* **2008**, *105*, 5075.
- Stradner, A.; Cardinaux, F.; Schurtenberger, P. *J. Phys. Chem. B* **2006**, *110*, 21222.
- Stradner, A.; Sedgwick, H.; Cardinaux, F.; Poon, W. C. K.; Egelhaaf, S. U.; Schurtenberger, P. *Nature* **2004**, *432*, 492.
- Stradner, A.; Thurston, G. M.; Schurtenberger, P. *J. Phys.: Condens. Matter* **2005**, *17*, S2805.
- Narayanan, J.; Liu, X. Y. *Biophys. J.* **2003**, *84*, 523.
- Velev, O. D.; Kaler, E. W.; Lenhoff, A. M. *Biophys. J.* **1998**, *75*, 2682.
- Gapinski, J.; Wilk, A.; Patkowski, A.; Häussler, W.; Banchio, A. J.; Pecora, R.; Nägele, G. *J. Chem. Phys.* **2005**, *123*, 054708.
- Zhang, F.; Skoda, M. W. A.; Jacobs, R. M. J.; Martin, R. A.; Martin, C. M.; Schreiber, F. *J. Phys. Chem. B* **2007**, *111*, 251.
- Zhang, F.; Skoda, M. W. A.; Jacobs, R. M. J.; Zorn, S.; Martin, R. A.; Martin, C. M.; Clark, G. F.; Weggler, S.; Hildebrandt, A.; Kohlbacher, O.; Schreiber, F. *Phys. Rev. Lett.* **2008**, *101*, 148101.
- Moon, Y. U.; Curtis, R. A.; Andersin, C. O.; Blanch, H. W.; Prausnitz, J. M. *J. Solution Chem.* **2000**, *29*, 699.
- Anderson, C. O.; Prausnitz, J. M.; Blanch, H. W. *Lawrence Berkeley National Laboratory* **2001**, November 10, 2001, LBNL49226. <http://repositories.cdlib.org/lbnl/LBNL>.
- Cremer, L. K.; Jimenez-Flores, R.; Richardson, T. *Trends Biotechnol.* **1988**, *6*, 163.
- Mine, Y. *Trends Food Sci. Technol.* **1995**, *6*, 225.
- Nicolai, T.; Pouzot, M.; Durand, D.; Weijers, M.; Visschers, R. W. *Europhys. Lett.* **2006**, *73*, 299.
- Weijers, M.; De Hoog, E. H. A.; Cohen Stuart, M. A.; Visschers, R. W.; Barneveld, P. A. *Colloids Surf., A* **2005**, *270–271*, 301.
- Weijers, M.; Visschers, R. W.; Nicolai, T. *Macromolecules* **2002**, *35*, 4753.
- Stein, P. E.; Leslie, G. W.; Finch, J. T.; McLauglin, D. J.; Carrell, R. W. *Nature* **1990**, *347*, 99.
- Matsumoto, T.; Chiba, J. *J. Chem. Soc., Faraday Trans.* **1990**, *86*, 2877.
- Matsumoto, T.; Inoue, H. *J. Colloid Interface Sci.* **1993**, *160*, 105.
- Proteins, Amino Acids, and Peptides*; Cohn, E. J., Edsall, J. T., Eds.; Reinhold Publishing Corp.: New York, 1943.
- Sztucki, M.; Narayanan, T.; Belina, G.; Moussaïd, A.; Pignon, F.; Hoekstra, H. *Phys. Rev. E* **2006**, *74*, 051504.
- Narayanan, T. Synchrotron small-angle X-ray scattering. In *Soft Matter: Characterization*; Borsali, R., Pecora, R., Eds.; Springer: Berlin, Heidelberg, 2008; Vol. II, p 899.
- Cernik, R. J.; Barnes, P.; Bushnell-Wye, G.; Dent, A. J.; Diakun, G. P.; Flaherty, J. V.; Greaves, G. N.; Heeley, E. L.; Helsby, W.; Jacques, S. D. M.; Kay, J.; Rayment, T.; Ryan, A.; Tang, C. C.; Terrill, N. J. *J. Synchrotron Radiat.* **2004**, *11*, 163.
- Keiderling, U.; Wiedenmann, A. *Physica B* **1995**, *213–214*, 895.
- Keiderling, U. *Appl. Phys. A* **2002**, *74*, S1455.
- Chen, S. H.; Lin, T. L. *Colloidal Solutions. In Neutron Scattering*; Price, D. L., Sköld, K., Eds.; Academic Press: London, 1987; Vol. 23 , Part B, p 489.
- Pedersen, J. S. *Adv. Colloid Interface Sci.* **1997**, *70*, 171.
- Chen, S. H. *Annu. Rev. Phys. Chem.* **1986**, *37*, 351.
- Glatter, O.; Kratky, O. *Small angle X-ray scattering*; Academic Press: London, 1982.
- Neutrons, X-rays and Light: Scattering Methods Applied to Soft Condensed Matter*; Lindner, P., Zemb, T., Eds.; Elsevier Science B. V.: Amsterdam, The Netherlands, 2002.
- Guinier, A.; Fournet, G. *Small Angle Scattering of X-rays*; John Wiley & Sons Ltd.: New York, 1955.
- Perkins, S. J.; Okemefuna, A. I.; Fernando, A. N.; Bonner, A.; Gilbert, H. E.; Furtado, P. B. *Methods Cell Biol.* **2008**, *84*, 376.
- Kline, S. R. *J. Appl. Crystallogr.* **2006**, *39*, 895.
- Hayter, J. B.; Penfold, J. *Mol. Phys.* **1981**, *42*, 109.
- Hansen, J. P.; Hayter, J. B. *Mol. Phys.* **1982**, *46*, 651.
- Jacrot, B. *Rep. Prog. Phys.* **1976**, *39*, 911.
- Stradner, A.; Cardinaux, F.; Schurtenberger, P. *Phys. Rev. Lett.* **2006**, *96*, 219801.
- Sciortino, F.; Mossa, S.; Zaccarelli, E.; Tartaglia, P. *Phys. Rev. Lett.* **2004**, *93*, 055701.
- Bloomfield, V. A. *Curr. Opin. Struct. Biol.* **1996**, *6*, 334.
- Olvera de la Cruz, M.; Belloni, L.; Delsanti, M.; Dalbiez, J. P.; Spalla, O.; Drifford, M. *J. Chem. Phys.* **1995**, *103*, 5781.
- Grosberg, A. Y.; Nguyen, T. T.; Shklovskii, B. I. *Rev. Mod. Phys.* **2002**, *74*, 329.